Stem Cell Research (2007) 1, 45–60

available at www.sciencedirect.com

www.elsevier.com/locate/scr

Differentiation is coupled to changes in the cell cycle regulatory apparatus of human embryonic stem cells

Adam A. Filipczyk [a,b], Andrew L. Laslett [b], Christine Mummery [a], Martin F. Pera [c,*]

[a] *Hubrecht Laboratory, Netherlands Institute for Developmental Biology and Stem Cell Research, Utrecht, The Netherlands*
[b] *Monash Institute of Medical Research, Monash University, and Australian Stem Cell Centre, Melbourne, Australia*
[c] *Center for Stem Cell and Regenerative Medicine, Keck School of Medicine, University of Southern California, Los Angeles, CA 90089-9720, USA*

Received 30 July 2007; received in revised form 31 August 2007; accepted 6 September 2007

Abstract Mouse embryonic stem cells (mESC) exhibit cell cycle properties entirely distinct from those of somatic cells. Here we investigated the cell cycle characteristics of human embryonic stem cells (hESC). HESC could be sorted into populations based on the expression level of the cell surface stem cell marker GCTM-2. Compared to mESC, a significantly higher proportion of hESC (GCTM-2$^+$ Oct-4$^+$ cells) resided in G_1 and retained G_1-phase-specific hypophosphorylated retinoblastoma protein (pRb). We showed that suppression of traverse through G_1 is sufficient to promote hESC differentiation. Like mESC, hESC expressed cyclin E constitutively, were negative for D-type cyclins, and did not respond to CDK-4 inhibition. By contrast, cyclin A expression was periodic in hESC and coincided with S and G_2/M phase progression. FGF-2 acted solely to sustain hESC pluripotency rather than to promote cell cycle progression or inhibit apoptosis. Differentiation increased G_1-phase content, reinstated cyclin D activity, and restored the proliferative response to FGF-2. Treatment with CDK-2 inhibitor delayed hESC in G_1 and S phase, resulting in accumulation of cells with hypophosphorylated pRb, GCTM-2, and Oct-4 and, interestingly, a second pRb$^+$ GCTM-2$^+$ subpopulation lacking Oct-4. We discuss evidence for a G_1-specific, pRb-dependent restriction checkpoint in hESC closely associated with the regulation of pluripotency.

Introduction

Terminal differentiation of progenitor cells is accompanied by irreversible exit from the cell cycle in the G$_1$ phase as the cells acquire their definitive phenotypic characteristics. Perhaps the best example of this intricate relationship is provided by the retinoblastoma (Rb) gene, a master regulator of G_1-S cell cycle traverse (Weinberg, 1995; reviewed in Classon and Harlow, 2002), which is the essential switch driving, for example, an undifferentiated myoblast toward the functional myotube. In these cells, cross talk between the muscle-specific transcription factor MyoD and phosphorylated Rb protein (pRb) initiates cell cycle shutdown in G_1 and promotes the downregulation of cyclins E and A. Dephosphorylation of pRb elevates MyoD levels further, leading to the upregulation of p21 in a positive feedback loop to block cell cycle progression. Together with the activation of the transcription factor MEF2 and other myogenic factors, pRb is essential for continued differentiation and cell cycle exit that culminate into full myogenesis (reviewed

* Corresponding author.
E-mail address: pera@usc.edu (M.F. Pera).

1873-5061/$ – see front matter © 2007 Elsevier B.V. All rights reserved.
doi:10.1016/j.scr.2007.09.002

in De Falco et al., 2006; Khidr and Chen, 2006). Recently, pRb and other "cell cycle" proteins have been implicated in the differentiation of many stem cell types, including those found in the eye lens, brain, peripheral nervous system, muscle, placenta, hematopoietic system, epidermis, melanocytes, hair cells, liver, prostate, lung, cerebellum, pituitary, and retina (reviewed in Skapek et al., 2006).

Pluripotent embryonic stem cells (ESC), in contrast to the progenitors, do not exit the cell cycle during their first differentiation steps. How control of their cell cycle is then related to differentiation is substantially less clear. Understanding the relationship is, however, essential if growth and differentiation are to be properly controlled. Mouse and primate ESC have been described previously as rapidly dividing with a truncated G_1 phase, lacking D-type cyclins and expressing permanently hyperphosphorylated pRb (Savatier et al., 1994; Stead et al., 2002; Fluckiger et al., 2006). Human ESC (hESC) have also been described as rapidly dividing with a truncated G_1 phase but, uniquely, these cells apparently also possess elevated expression of cyclin D2 and CDK-4 mRNA, a feature characteristic of human ESC and often interpreted as the responsiveness of hESC to growth factor signaling in G_1 (Becker et al., 2006, 2007).

Derived from the pluripotent cells in the inner cell mass of the preimplantation blastocyst, both mouse and human ES cells are in principle karyotypically normal, can be propagated indefinitely, and can differentiate into cell types representative of all three embryonic germ layers (Pera et al., 2000). ES cells from both species express a set of genes characteristic of the pluripotent state, including the transcription factors Nanog and Oct-4 (Pera and Trounson, 2004). In the absence of mouse embryonic fibroblast (MEF) feeder cells, mouse ES cells can be maintained in culture and cloned with high efficiency in the presence of leukemia inhibitory factor (LIF) (Smith et al., 1988; Williams et al., 1988). MEF feeders also inhibit the differentiation of hESC, but LIF does not support hESC self-renewal (Thomson et al., 1998) and the cloning efficiency of these cells is very poor (<1%) (Amit et al., 2000). HESC appear to benefit from basic fibroblast growth factor (FGF-2) supplementation under serum-free conditions (Amit et al., 2000; Xu et al., 2005) but it is not clear whether FGF-2 acts directly on hESC to stimulate proliferation, inhibit differentiation, and/or prevent apoptosis or whether its effect is mediated in part through feeder cells (Dvorak et al., 2005; Greber et al., 2007). Thus, while ES cells from mouse or human share attributes associated with pluripotency, they appear to display different requirements for maintenance and growth *in vitro*.

In this study we examined the cell-cycle characteristics of hESC and documented changes in cell-cycle events that accompanied their differentiation. Interestingly, contrary to previous accounts, hESC, like mESC, were negative for cyclin D proteins and unresponsive to CDK-4 inhibitor treatment. All stem cell marker-positive cells were cyclin E positive, indicating constitutive expression, while cyclin A was periodically expressed, coinciding with cell progression through S and G_2/M phases. Importantly, we found the hypophosphorylated form of pRb present in hESC and expressed in the G_1 phase of the cell cycle. The mode of cell cycle control in hESC appears to be different from that of other pluripotent cell types documented so far. Spontaneous differentiation extended the G_0/G_1 phase, restored D-type cyclin activity, lowered the expression of the CDK-2 kinase partners cyclins E and A, and increased pRb activation. To examine whether cycle perturbation could promote hESC differentiation, we treated hESC with a CDK-2-specific inhibitor and successfully delayed these cells in the G_0/G_1 and G_2/M phases of the cell cycle. This resulted in the accumulation of hESC positive for the G_1-specific, hypophosphorylated form of pRb, and interestingly, we also found a significant increase in a cell subpopulation positive for hypophosphorylated pRb and GCTM-2, which had lost Oct-4. We discuss evidence for a unique, functional pRb-dependent restriction checkpoint in the hESC G_1 phase and its role in specifying the choice between self-renewal and differentiation. In light of these findings we also examine further the biological effects of FGF-2 in hESC cultures.

Results

Serum-free culture of hESC on MEF with FGF-2

HESC culture on MEF in serum-free medium supplemented with FGF-2 (4 ng/ml) has been described previously (Amit et al., 2000). We confirmed the long-term (>30 passages) propagation of the hESC lines HES-2, HES-3, and HES-4 using this serum-free culture system. Under these conditions, each cell line retained typical hESC morphology (Supplementary Figs. 1a and 1b). Immunocytochemical analysis with antibodies against Oct-4 and the cell surface proteoglycan characteristic of primate pluripotent stem cells (GCTM-2 and TRA-1-60) showed that all lines also retained stem cell marker expression (Supplementary Figs. 1c–1h) and normal karyotypes (Supplementary Figs. 1i and 1j), though in some serum-free-grown cultures we have observed the emergence of aneuploid variants (unpublished data), similar to previous observations (Draper et al., 2004). These aneuploid cultures were not included in this study. The cell lines used for this study retained the ability to form teratomas in SCID mice containing tissues representative of each of the three embryonic germ layers (data not shown).

Figure 1 (a) Flow-cytometric profile showing expression of the hESC marker GCTM-2. Cells within the profile are subdivided into three subpopulations: GCTM-2^{NEG}, GCTM-2^{LOW}, and GCTM-2^{HIGH} cells. For each gated population, cell proportions in G_0/G_1, S, and G_2/M phases of the cell cycle are quantified and represented graphically. Significant differences are indicated by asterisks (**$p<0.01$). (b) Double-label flow-cytometric analysis showing the proportions of GCTM-2^{NEG}, GCTM-2^{LOW}, and GCTM-2^{HIGH} cells colabeling with the stem cell marker Oct-4. Significant differences are indicated by asterisks (**$p<0.01$). (c) Flow-cytometric profile showing expression of the mouse ES cell marker SSEA-1. Cells within the profile are subdivided into three subpopulations: SSEA-1^{NEG}, SSEA-1^{LOW}, and SSEA-1^{HIGH} cells. For each gated population, cell proportions in G_0/G_1, S, and G_2/M phases of the cell cycle are quantified and represented in a bar graph. There were no significant differences.

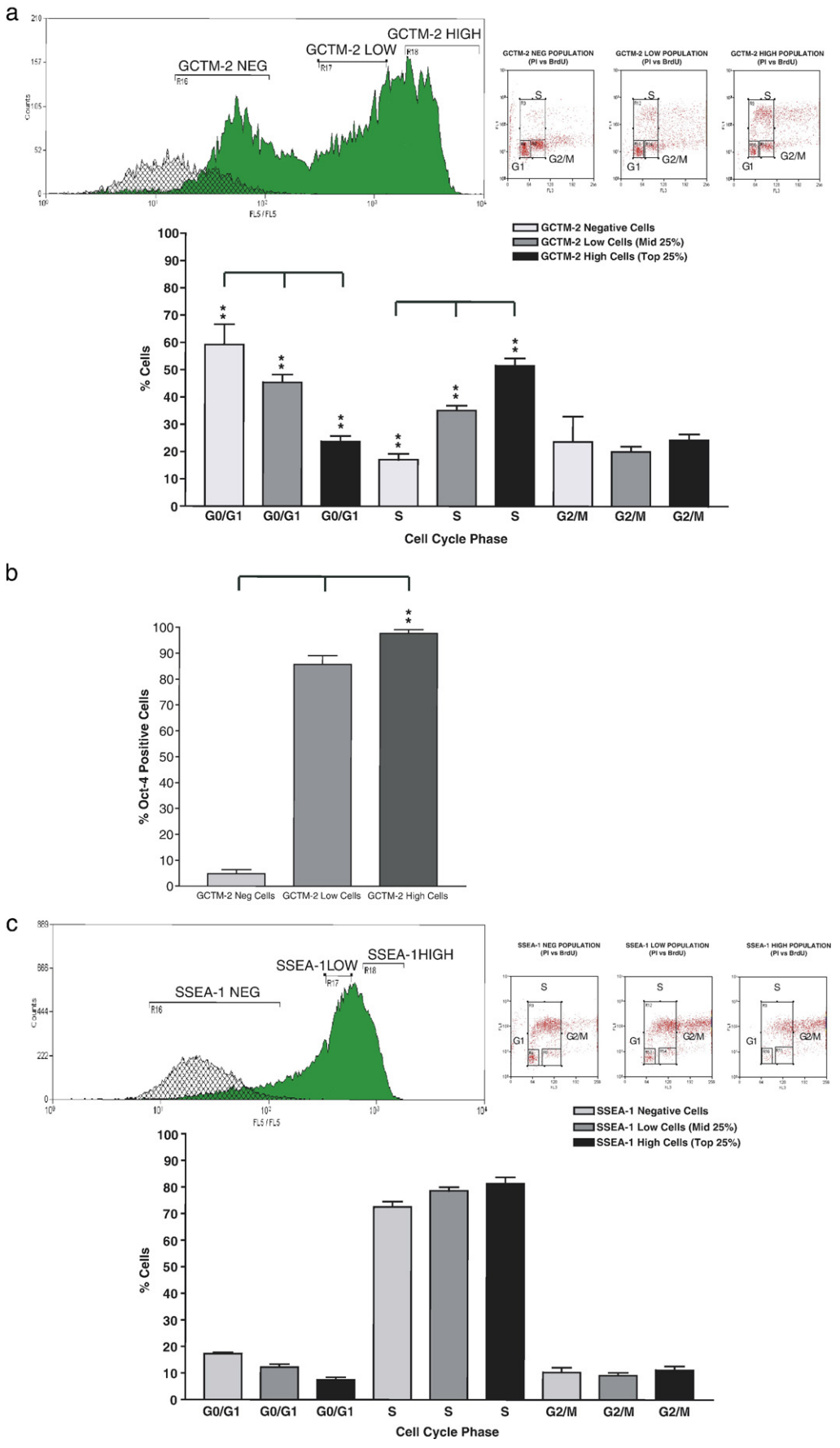
a
GCTM-2 NEG
GCTM-2 LOW
GCTM-2 HIGH
R16
R17
R18
Counts
FL5 / FL5
GCTM-2 NEG POPULATION (PI vs BrdU)
GCTM-2 LOW POPULATION (PI vs BrdU)
GCTM-2 HIGH POPULATION (PI vs BrdU)
S
G1
G2/M
GCTM-2 Negative Cells
GCTM-2 Low Cells (Mid 25%)
GCTM-2 High Cells (Top 25%)
% Cells
G0/G1 G0/G1 G0/G1 S S S G2/M G2/M G2/M
Cell Cycle Phase
b
% Oct-4 Positive Cells
GCTM-2 Neg Cells
GCTM-2 Low Cells
GCTM-2 High Cells
c
SSEA-1 NEG
SSEA-1LOW
SSEA-1HIGH
SSEA-1 NEG POPULATION (PI vs BrdU)
SSEA-1 LOW POPULATION (PI vs BrdU)
SSEA-1 HIGH POPULATION (PI vs BrdU)
SSEA-1 Negative Cells
SSEA-1 Low Cells (Mid 25%)
SSEA-1 High Cells (Top 25%)
% Cells
G0/G1 G0/G1 G0/G1 S S S G2/M G2/M G2/M
Cell Cycle Phase

Marker and cell cycle heterogeneity within hESC cultures

To define the cell cycle structure of hESC we developed a flow-cytometric immunoassay simultaneously measuring the proportions of cells in G_0/G_1, S, and G_2/M phases of the cell cycle (5-bromo-2 and prime;-deoxyuridine (BrdU) incorporation vs propidium iodide (PI) staining) and labeling intensity for the hESC marker GCTM-2. This enabled the comparison of cell cycle profiles in subpopulations of cells with different levels of marker expression. To ensure that MEF feeder cell contamination was minimal we quantitated cells labeling positive for the mouse fibroblast marker Thy-1.2. The proportion of MEF feeders in samples analyzed did not exceed 4.2 ± 2.1% (Supplementary Fig. 2). We analyzed cell subpopulations that were negative (GCTM-2^{NEG}; relative to isotype-specific primary control), weakly positive (GCTM-2^{LOW}; cells ± 12.5% from the mean fluorescence intensity, representing cells losing marker expression and thus differentiating), and strongly positive (GCTM-2^{HIGH}; cells in the top 25% of GCTM-2 labeling distribution, a fraction in which all cells coexpress Oct-4) (Fig. 1a). The three cell populations had significantly different proliferative fractions (S-phase cells) as indicated by BrdU incorporation. The GCTM-2^{HIGH} population had the highest proportion of S-phase cells (52 ± 4.6%) and the lowest proportion of cells in G_0/G_1 (24 ± 3.4%). The GCTM-2^{LOW} population had a significantly lower proportion of cells in S phase (35 ± 3.1%), while the percentage of cells in G_0/G_1 was larger (45.3 ± 4.9%). The population lacking GCTM-2 expression (GCTM-2^{NEG} cells) had the lowest S-phase fraction (17 ± 3.8%) and the highest proportion of cells in G_0/G_1 (59.3 ± 12.5%). No significant differences between the three subpopulations were observed in the proportions of cells in G_2/M (23 ± 16, 20 ± 3.4, 24.2 ± 3.8%). Double-label flow-cytometric analysis experiments using GCTM-2 and Oct-4 confirmed that 98 ± 1.4% of GCTM-2^{HIGH} cells were Oct-4 positive (Fig. 1b). The GCTM-2^{LOW} and GCTM-2^{NEG} cell subpopulations contained significantly lower (85 ± 3.3 and under 5%, respectively) proportions of Oct-4-positive cells. GCTM-2^{HIGH} cells thus represent a subpopulation uniformly expressing Oct-4 and other markers of hESC.

For comparison the mouse ES cell cycle was analyzed by the same method after fractionation of the population according to the intensity of the mouse ES cell marker SSEA-1. We analyzed cells that were negative (SSEA-1^{NEG}; relative to isotype-specific primary control), weakly positive (SSEA-1^{LOW}; cells in the mid-25% of SSEA-1 labeling distribution), and strongly positive (SSEA-1^{HIGH}; cells in the top 25% of SSEA-1 labeling distribution) for their cell cycle stage distribution (Fig. 1c). Mouse ES cells (SSEA-1^{HIGH}) had a different cell cycle structure compared to their human counterparts (GCTM-2^{HIGH} cells), with 81 ± 4.1% of cells in S phase and only low cell proportions in G_0/G_1 (8 ± 1.7%) and G_2/M (11 ± 0.8%) phases, as previously described (Savatier et al., 1994, 1996, 2002; Stead et al., 2002). The SSEA-1^{LOW} and SSEA-1^{NEG} cells displayed a progressive reduction in the S-phase fraction and an increase in the G_0/G_1 fraction, although no significant cell cycle differences were observed between the three subpopulations.

Differentiation inversely changes the expression of G_1- and S-phase-promoting cyclins in hESC cultures

HESC grown on MEF for 7 days in serum-free medium with FGF-2 were stained for stem cell marker Oct-4 and cyclins D1, D2, D3, E, or A by indirect double immunocytochemistry. Spontaneously differentiated, Oct-4-negative human cells were distinguished from MEF by their distinct nuclear morphology when counterstained with the nuclear dye Hoechst 33248. Human Oct-4-positive cells were uniformly negative for cyclin D1 (Figs. 2a–2d), cyclin D2 (Figs. 2f–2i), and cyclin D3 (Figs. 2o–2r). However, 99 ± 1.0% of Oct-4-positive cells costained with cyclin E in the nucleus and cytoplasm (Figs. 3a–3e) and 60 ± 1.5% costained with cyclin A only in the nucleus (Figs. 4a–4e).

In the population of differentiated human cells (Oct-4-negative cells that showed loss of hESC morphology), 23 ± 7.3% expressed cyclin D1 (Figs. 2a–2e), 22 ± 5.4% expressed cyclin D2 (Figs. 2j–2n), and 32 ± 4.1% stained with an antibody to cyclin D3 (Figs. 2s–2w). In all cells D-type cyclins were localized to the nucleus. Cyclin E was present in 19 ± 3.6% of Oct-4-negative cells (Fig. 3e) and the cyclin A antibody stained 18 ± 7.9% (Fig. 4e). In both cases the staining was faint and mostly nuclear. Thus, hESC lack D-type cyclins, and the expression of these proteins is switched on upon differentiation, as in mESC. The high cycling fraction of hESC compared to differentiated cells is associated with the expression of cyclins E and A, and the lower S-phase fraction of differentiated cells is coupled with a reduction in the proportion of cells positive for these cyclins. Using a flow-cytometric immunoassay we determined the association of cyclin A expression with cell cycle phase (PI-counterstained nuclei) for both GCTM-2^{HIGH} and GCTM-2^{NEG} cells (Fig. 4f). In both cell fractions the mode of cyclin A expression was identical, rising during S and G_2 phases followed by downregulation in M phase and absence in G_0/G_1. In accordance with quantitative analysis performed on Oct-4-positive and Oct-4-negative cells by indirect immunofluorescence, the GCTM-2^{HIGH} cell fraction contained a significantly higher proportion of cells positive for cyclin A (50 ± 3.4%) compared to the GCTM-2^{NEG} cell fraction (18 ± 5.6%) (Fig. 4f).

Figure 2 Double immunofluorescence staining for D-type cyclins and Oct-4 showing (a) hESC and adjoining differentiated cells (phase contrast), (b) corresponding Oct-4 expression (red), (c) Hoechst 33342 nuclear staining (blue), and (d) cyclin D1 staining (green) and (e) quantification of Oct-4-positive and -negative cells expressing cyclin D1 in hESC cultures. (f) HESC (phase contrast), (g) corresponding Oct-4 expression (red), (h) Hoechst 33342 nuclear staining (blue), and (i) cyclin D2 staining (green), (j) differentiated cells (k) negative for Oct-4 expression (red), (l) Hoechst 33342 nuclear staining (blue), and (m) cyclin D2 presence (green) and (n) quantification of Oct-4-positive and -negative cells expressing cyclin D2 in hESC cultures. (o) HESC (phase contrast), (p) corresponding Oct-4 expression (red), (q) Hoechst 33342 nuclear staining (blue), and (r) cyclin D3 staining (green), (s) differentiated cells (t) negative for Oct-4 expression (red), (u) Hoechst 33342 nuclear staining (blue), and (v) cyclin D3 presence (green) and (w) quantification of Oct-4-positive and -negative cells expressing cyclin D3 in hESC cultures. Scale bars, 100 μm.

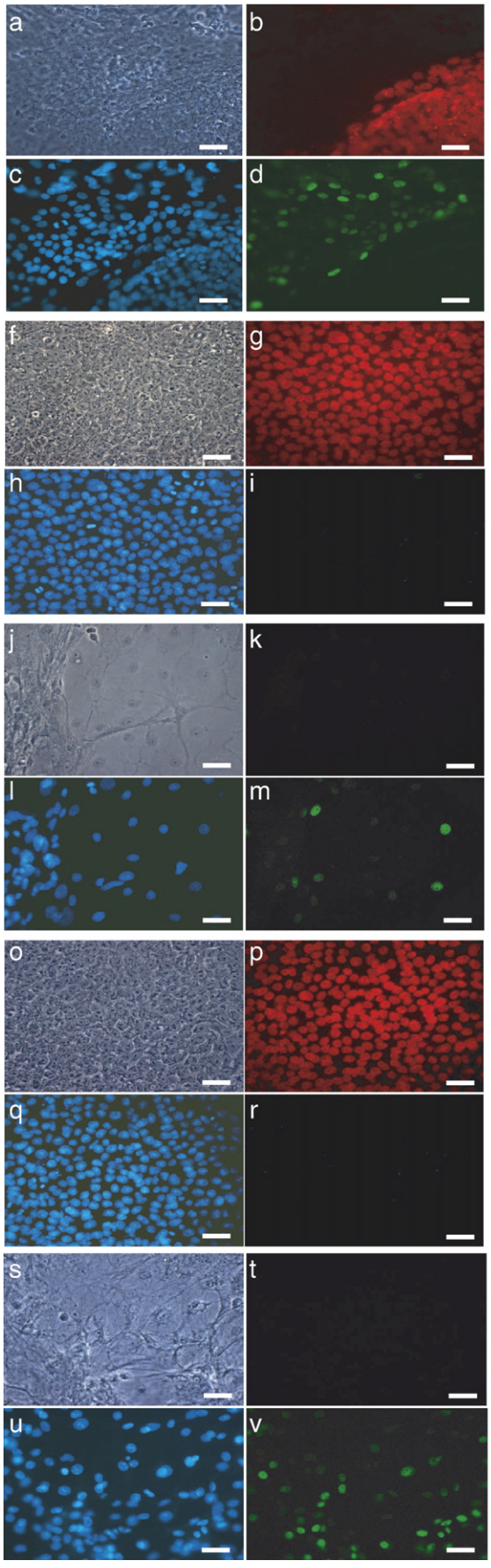
a
b
c
d
f
g
h
i
j
k
l
m
o
p
q
r
s
t
u
v

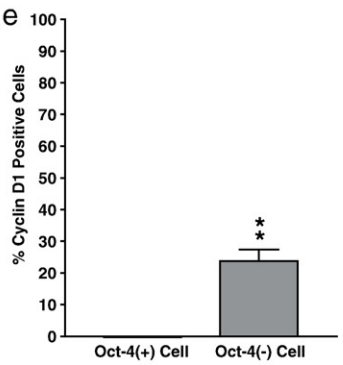
e
% Cyclin D1 Positive Cells
100
90
80
70
60
50
40
30
20
10
0
**
Oct-4(+) Cell
Oct-4(-) Cell

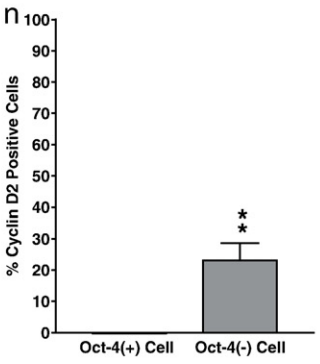
n
% Cyclin D2 Positive Cells
100
90
80
70
60
50
40
30
20
10
0
**
Oct-4(+) Cell
Oct-4(-) Cell

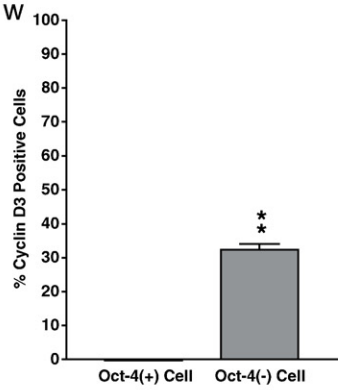
w
% Cyclin D3 Positive Cells
100
90
80
70
60
50
40
30
20
10
0
**
Oct-4(+) Cell
Oct-4(-) Cell

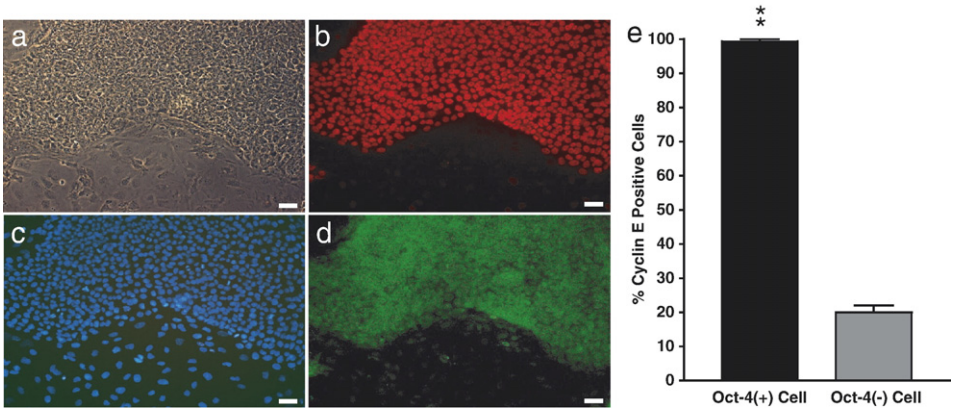

Figure 3 Double immunofluorescence staining for cyclin E and Oct-4 showing (a) human ES and differentiated cells, (b) corresponding Oct-4 expression (red), (c) Hoechst 33342 nuclear staining (blue), (d) cyclin E staining for both cell types (green), and (e) quantification of Oct-4-positive and -negative cells expressing cyclin E in hESC cultures. Scale bars, 100 μm.

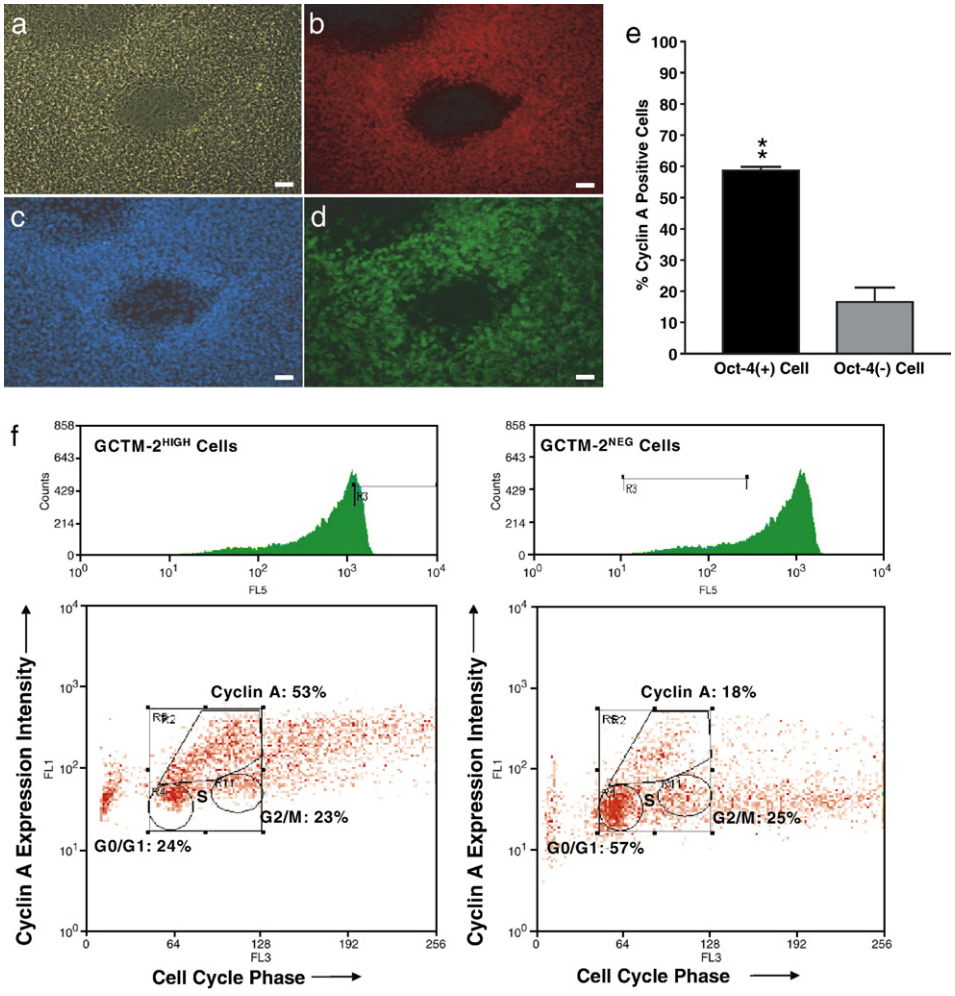

Figure 4 Double immunofluorescence staining for cyclin A and Oct-4 showing (a) human ES and differentiated cells (phase contrast), (b) corresponding Oct-4 expression (red), (c) Hoechst 33342 nuclear staining (blue), (d) cyclin A staining across both cell types (green), and (e) quantification of Oct-4-positive and -negative cells expressing cyclin A in hESC cultures. (f) Flow-cytometric analysis of cyclin A expression versus nuclear staining intensity for GCTM-2^{HIGH} and GCTM-2^{NEG} cells. Both cell subpopulations show cyclin A staining consistent with a steady upregulation during S and G_2 phases followed by downregulation at M phase and absence of expression in G_0/G_1. Scale bars, 100 μm.

pRb undergoes a G_1-specific dephosphorylation event in hESC

Another property, which has been correlated with the fast proliferation and truncated G_1 of mouse ES cells, is the absence of hypophosphorylated pRb protein (Savatier et al., 1994). In somatic cells pRb is reversibly hyperphosphorylated in S and G_2/M phases and becomes hypophosphorylated at the end of M phase and during most of the G_1 phase (Buchkovich et al., 1989). We asked if hypophosphorylated pRb protein was present in hESC (GCTM-2^{HIGH} cells) that were shown to have the highest proliferative fraction and the smallest cell fraction with 2*N* DNA content (G_0/G_1 cells). Immunosorted GCTM-2^{HIGH} cell lysates were examined by

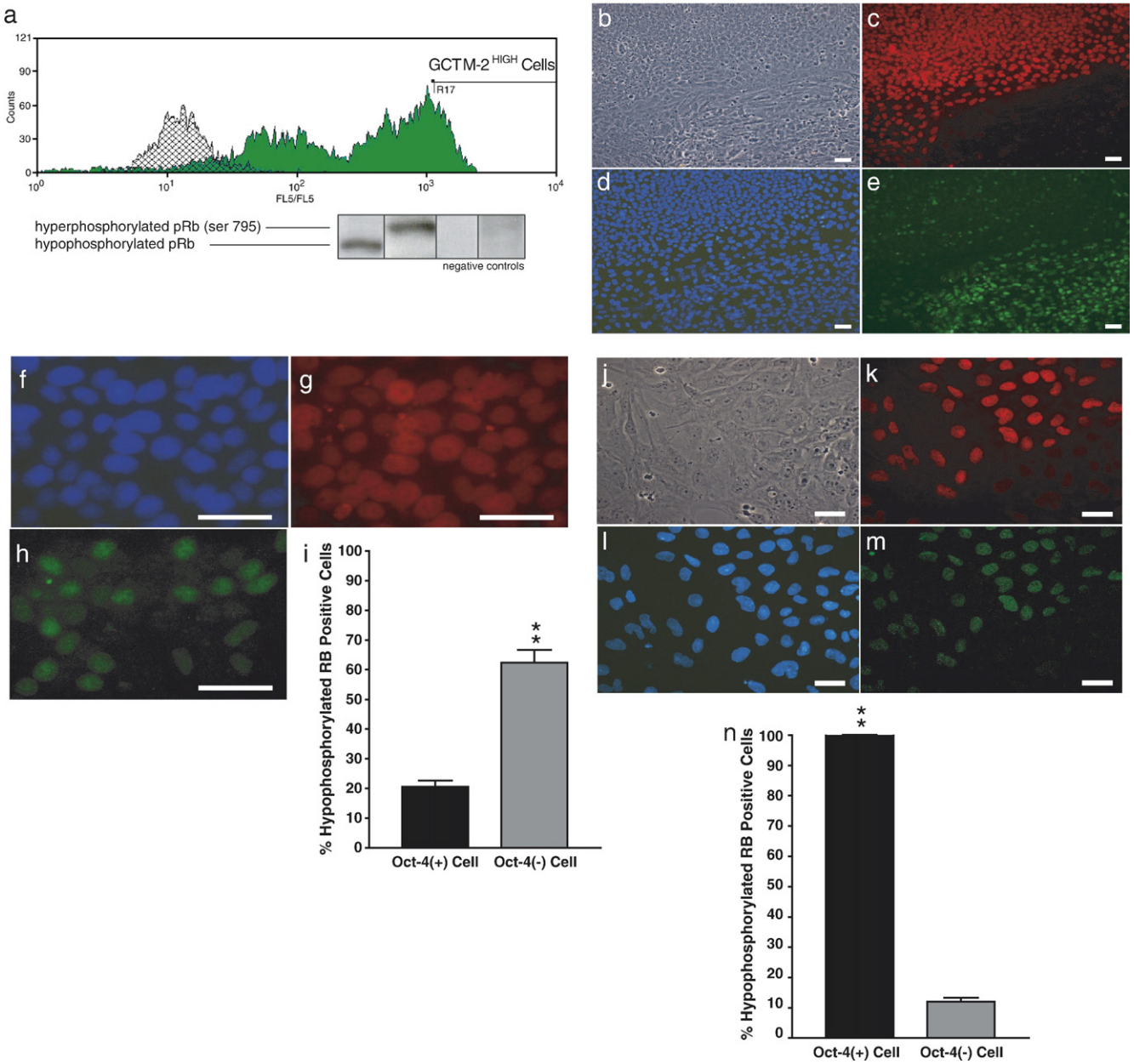

Figure 5 (a) Immunosorted GCTM-2^{HIGH} cells were used for an immunoblot analysis showing the presence of both hypophosphorylated and hyperphosphorylated pRb (Ser795) protein species. Double immunofluorescence staining for hypophosphorylated Rb protein and Oct-4 showing (b) human ES and differentiated cells (phase contrast), (c) corresponding Oct-4 expression (red), (d) Hoechst 33342 nuclear staining (blue), and (e) hypophosphorylated pRb staining across both cell types (green). Oil immersion photographs (63 and times;) showing (f) hESC nuclei stained with Hoechst 33342 (blue), (g) cells positive for stem cell marker Oct-4 (red), and (h) nuclear staining for hypophosphorylated pRb protein (green). (i) Quantification of Oct-4-positive and -negative cells expressing hypophosphorylated pRb in hESC cultures. Scale bars, 100 μm. Double immunofluorescence staining for hyperphosphorylated pRb (Ser 795) and Oct-4 showing (j) human ES and differentiated cells, (k) corresponding Oct-4 expression (red), (l) Hoechst 33342 nuclear staining (blue), and (m) hyperphosphorylated pRb staining for both cell types (green). Scale bars, 100 μm. (n) Quantification of Oct-4-positive and -negative cells expressing hyperphosphorylated pRb in hESC cultures.

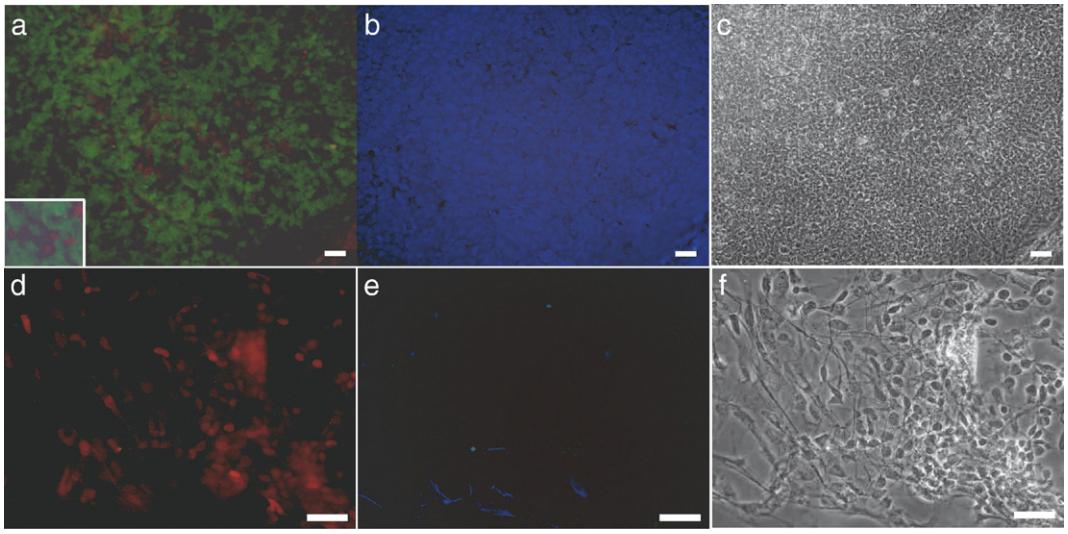

Figure 6 Triple label immunofluorescence showing (a) the mutual exclusion of cyclin A positivity (green) and the presence of hypophosphorylated pRb protein (red) on (b) hESC identified by positivity for GCTM-2 (blue) and (c) ES cell morphology. The same analysis was performed on differentiated human cells showing (d) the absence of cyclin A staining (green), the majority of cells positive for hypophosphorylated pRb (red) and (e) the lack of GCTM-2 expression, (f) accompanied by a differentiated cell morphology. Scale bars, 100 μm.

immunoblot analysis using two different monoclonal antibodies: pRb-Ser 795, which detects pRb hyperphosphorylated by cyclinE/CDK-2 or cyclin A/CDK-2 complexes (Zarkowska and Mittnacht, 1997), and pMG99-549, which recognizes the hypophosphorylated form characteristic of early G1 cells (Juan et al., 1998). These immunoreagents detected both isoforms of pRb in GCTM-2^{HIGH} hESC (Fig. 5a). Immunofluorescence analysis using pMG99-549 (Figs. 5b–5h) and pRb-Ser 795 (Figs. 5j–5m) antibodies detected 20±3.7% (Fig. 5i) and 99.9±0.1% (Fig. 5n) of cells, respectively, also positive for Oct-4. 65±4.5% of differentiated (Oct-4-negative) human cells were positive for hypophosphorylated pRb (Fig. 5i) and incidentally had the highest percentage of cells in G_1, as previously shown by cell cycle distribution analysis (GCTM-2^{NEG} cells). Only 12±2.1% of Oct-4-negative human cells were positive for hyperphosphorylated pRb (Fig. 5n), as expected of cells predominantly residing in G_0/G_1. Given that cyclin A expression is associated with the S and G_2/M phases of the cell cycle in both GCTM-2^{HIGH} and GCTM-2^{NEG} cells, we expected that the presence of a G_1-specific hypophosphorylated form of pRb should never coincide with cyclin A-positive cells. Indirect triple immunocytochemistry analysis confirmed that cells positive for GCTM-2 and hypophosphorylated pRb were all negative for cyclin A (Figs. 6a–6c). The expression of hypophosphorylated pRb and cyclin A in cells negative for GCTM-2 were also mutually exclusive (Figs. 6d–6f).

Induction of G_1-S delay in hESC upregulates dephosphorylated pRb and promotes the loss of Oct-4 in hESC cultures

The above findings showed that hESC have a unique mode of cell cycle control whereby the lack of D-type cyclins is accompanied by a significant G_0/G_1 cell fraction. The

Figure 7 (a) Colony size and cell morphology of hESC treated for 6 days with DMSO or (b) Roscovitine (RV; 30 μM) CDK-2 inhibitor. (c) Cell cycle distribution analysis of GCTM-2^{HIGH} cells after 6 days of treatment with DMSO (gray bars) or RV (30 μM) (hatched bars). The proportion of RV-treated cells in G_0/G_1 was significantly higher (*$p<0.05$) compared to the proportion of DMSO control cells at day 6. The proportion of RV-treated cells in G_2/M was significantly lower (*$p<0.05$) compared to the proportion of DMSO control cells at day 6. (d) Cell cycle profile of DMSO-treated control hESC at day 6 showing distributions of cells in G_0/G_1, S, and G_2/M phases. (e) Cell cycle profile of RV-treated hESC at day 6 showing the accumulation of cells in G_0/G_1 and S, with a significantly lower proportion of cells remaining in G_2/M. (f) The percentages of GCTM-2-positive cells under the DMSO and RV treatment conditions after 6 days of culture showing no significant change in the percentage of proteoglycan-positive cells. Colony size and cell morphology of hESC treated for 6 days with (g) DMSO or (h) CDK-4 inhibitor II (1,4-dimethoxy-9-thio(10*H*)-acridone, 10 μM). (i) Cell cycle distribution analysis of GCTM-2^{HIGH} cells after 6 days of treatment with DMSO (gray bars) or CDK-4 inhibitor II (10 μM) (hatched bars). The proportions of CDK-4 inhibitor II-treated cells in G_0/G_1, S, and G_2/M were not significantly different compared to the proportions of DMSO control cells at day 6. (j) Cell cycle profile of DMSO-treated control hESC at day 6 showing distributions of cells in G_0/G_1, S, and G_2/M phases. (k) Cell cycle profile of CDK-4 inhibitor II-treated hESC at day 6 showing no change in cell cycle distribution. (l) The percentages of GCTM-2 positive cells under the DMSO and CDK-4 inhibitor II treatment conditions after 6 days of culture showing no significant change in the percentage of proteoglycan-positive cells. (m) Triple immunolabeling for GCTM-2 (orange), Oct-4 (blue), and hypophosphorylated retinoblastoma under the DMSO and (n) RV treatment conditions after 6 days of growth. Scale bars, 100 μm. (o) RV treatment yielded a significantly higher (**$p<0.01$) proportion of GCTM-2/Oct-4 double-positive hESC expressing the G_1-specific, hypophosphorylated form of pRb at day 6 and (p) produced a significantly higher (**$p<0.01$) proportion of hypophosphorylated pRb-expressing cells positive for GCTM-2 but negative for Oct-4.

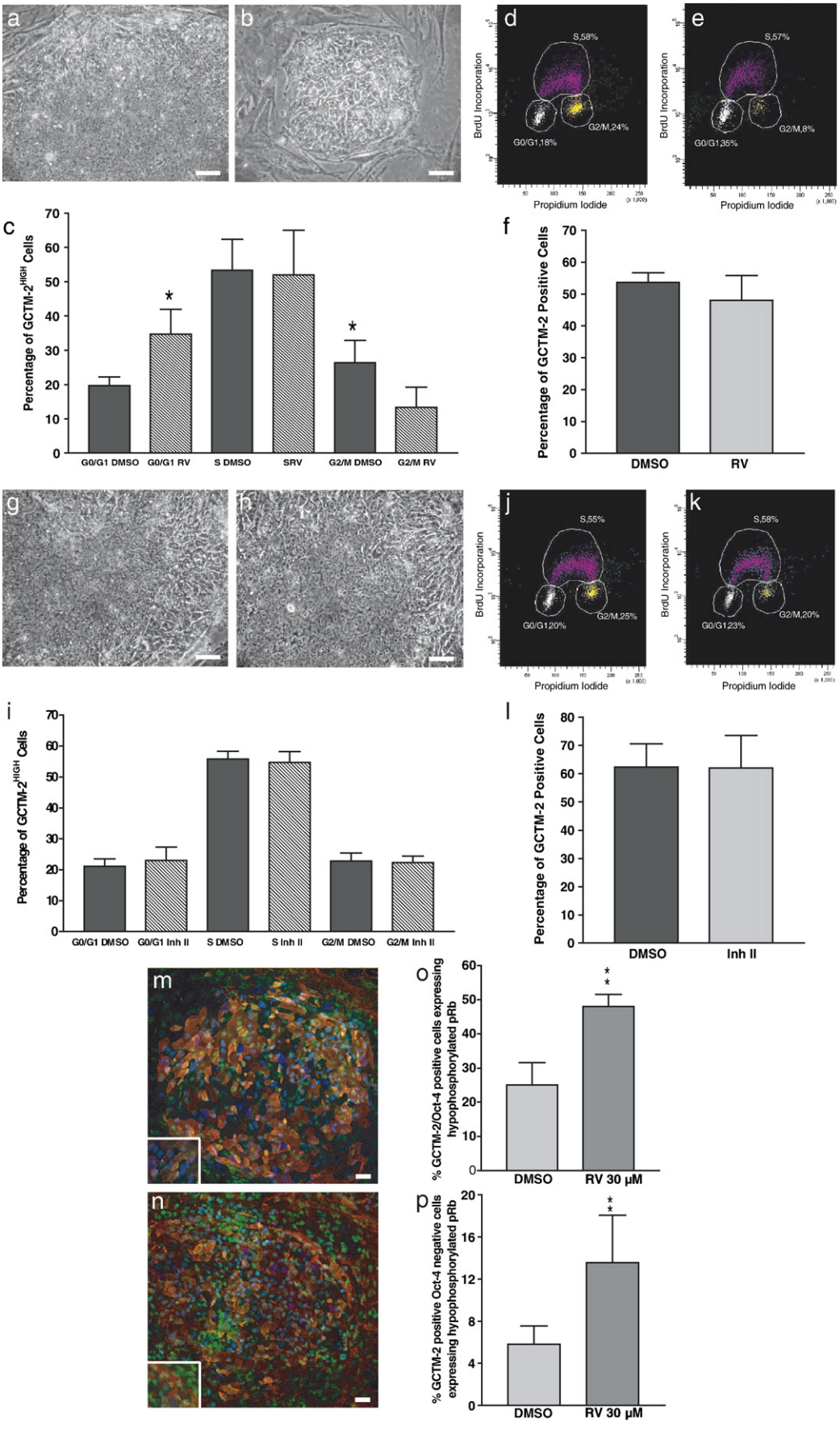
a
b
d
S,58%
G2/M,24%
G0/G1,18%
BrdU Incorporation
Propidium Iodide
e
S,57%
G2/M,8%
G0/G1,35%
BrdU Incorporation
Propidium Iodide
c
Percentage of GCTM-2HIGH Cells
G0/G1 DMSO
G0/G1 RV
S DMSO
SRV
G2/M DMSO
G2/M RV
f
Percentage of GCTM-2 Positive Cells
DMSO
RV
g
h
j
S,55%
G2/M,25%
G0/G120%
BrdU Incorporation
Propidium Iodide
k
S,58%
G2/M,20%
G0/G123%
BrdU Incorporation
Propidium Iodide
i
Percentage of GCTM-2HIGH Cells
G0/G1 DMSO
G0/G1 Inh II
S DMSO
S Inh II
G2/M DMSO
G2/M Inh II
l
Percentage of GCTM-2 Positive Cells
DMSO
Inh II
m
n
o
% GCTM-2/Oct-4 positive cells expressing hypophosphorylated pRb
DMSO
RV 30 μM
p
% GCTM-2 positive Oct-4 negative cells expressing hypophosphorylated pRb
DMSO
RV 30 μM

expression of cyclins E/A indicates a dependence on CDK-2 kinase for passage through the R point, defined by pRb rephosphorylation before completion of the G_1-S traverse. We proceeded to test this model further by asking if hESC could be delayed at the G_1-S border by the administration of a CDK-2-specific pharmacological inhibitor. HESC cultures were grown for 6 days in medium supplemented with the pharmacological CDK-2 inhibitor Roscovitine (RV; 30-μM, IC_{50}

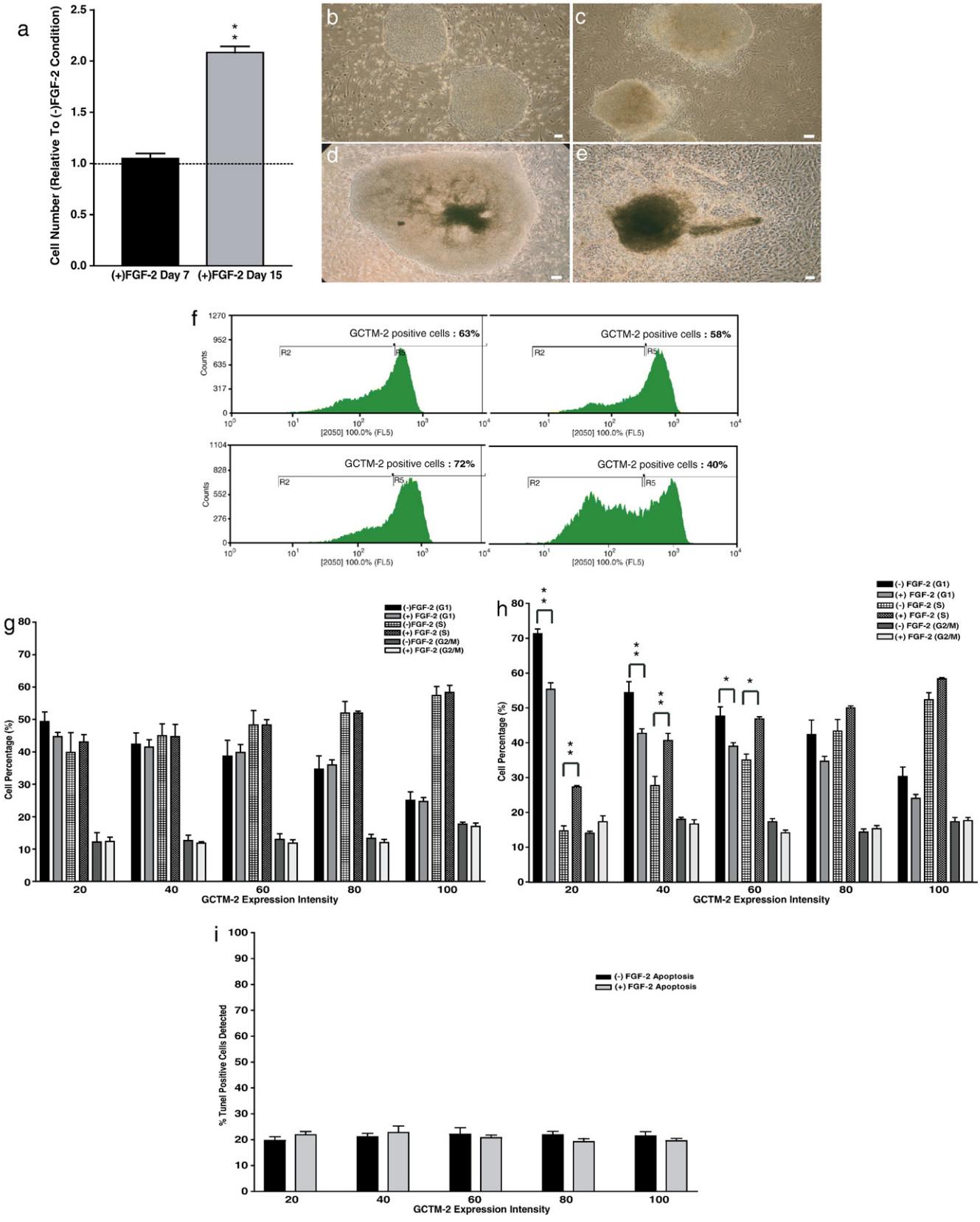

700 nM) or DMSO carrier and analyzed for cell cycle structure by flow-cytometric immunoassay.

After 6 days of growth, the RV-treated cultures displayed visibly smaller hESC colonies compared to the DMSO-treated control (Figs. 7a and 7b). Flow-cytometric analysis showed that the RV-treated GCTM-2^{HIGH} subpopulation retained a significantly higher proportion of cells in G_0/G_1 (34 ± 2.5%) compared to the DMSO condition (19 ± 3.2%) (Figs. 7c–7e). The proportion of S-phase GCTM-2^{HIGH} cells between RV and DMSO treatments was not significantly different, while the percentage of cells in G_2/M was significantly lower in RV-treated GCTM-2^{HIGH} cells (8 ± 3.6%) compared to the control (18 ± 4.5%) (Figs. 7c–7e). After 6 days of inhibitor treatment, no significant differences in the proportions of GCTM-2-positive cells were observed between RV-(52 ± 3.1%) and DMSO-(46 ± 3.5%) treated cultures (Fig. 7f). Consistent with the absence of cyclin D1, D2, and D3 expression, no significant effect on GCTM-2^{HIGH} cell cycle structure or GCTM-2-positive cell content was observed after 6 days of treatment with the pharmacological CDK-4 inhibitor II (1,4-dimethoxy-9-thio(10*H*)-acridone at 10 μM, IC_{50} 200 nM) compared to carrier treatment alone (Figs. 7g–7l). By contrast the same CDK-4 inhibition significantly delayed the GCTM-2^{NEG} cell subfraction in G_1 compared to carrier-treated cells, reinforcing our conclusions that differentiation restores CDK-4 dependency and activates restriction point control (Supplementary Fig. 3). Treatment of MEF cells with CDK-4 inhibitor II for 48 h also resulted in a significant delay of cells in G_1 compared to carrier-treated cells (Supplementary Fig. 4).

We next performed indirect triple immunostaining and confocal imaging for the hypophosphorylated form of pRb together with stem cell markers GCTM-2 and Oct-4 on hESC cultures treated for 6 days with RV or DMSO. Reflecting the significantly higher GCTM-2^{HIGH} G_0/G_1 cell content after RV treatment, the inhibitor also significantly increased the proportion of GCTM-2/Oct-4 double-positive cells expressing the hypophosphorylated form of pRb protein by twofold (Figs. 7m–7o) (48 ± 3.3%) compared to the untreated control (24 ± 6.5%). Confocal imaging analysis of DMSO- or RV-treated hESC colonies showed the presence of cells double positive for GCTM-2 and hypophosphorylated pRb that had lost Oct-4 expression (Figs. 7m and 7n). We quantified the number of these cells under either condition and found that RV treatment yielded a significantly higher proportion of cells positive for the G_1-specific, hypophosphorylated form of pRb, which retained the Oct-4-negative, GCTM-2-positive immunophenotype (14.8 ± 3.3%), compared to DMSO treatment alone (6.3 ± 0.9%) (Fig. 7p). Inhibiting G_1 phase transition was therefore sufficient to initiate the onset of differentiation.

Varying biological effects of FGF-2 on cell subpopulations in hESC cultures

The existence of a significant G_1 phase in hESC, along with a potential regulatory mechanism in the form of cyclin A and pRb, suggested that in contrast to mESC, mitogens might act on these cells to regulate the G_1/S phase transition. FGF-2 facilitates the clonal derivation of hESC lines and supports their maintenance in serum-free medium (Amit et al., 2000; Xu et al., 2005). Further work has shown that FGF-2 and its receptors are expressed in hESC (Dvorak et al., 2005) and that the factor stimulates the secretion of beneficial molecules in MEF that support hESC in culture while suppressing the release of differentiation-inducing activity (Greber et al., 2007). However, the possibility that FGF-2 modulates other biological effects on hESC has not been examined. We cultured hESC on MEF under serum-free conditions with or without FGF-2 (4 ng/ml) supplementation for short-term (7 days) and prolonged (15 days) culture periods. We found no difference at experimental day 6 between the numbers of colonies formed from cell clumps passaged into medium with (2670 colonies) or without FGF-2 (2625 colonies). We next determined the number of cells present at day 7 and day 15 in FGF-2-treated and untreated cultures. No differences in vital cell numbers were observed between the two conditions at day 7; however, in the presence of FGF-2 the number of live cells at day 15 was over twofold higher than in untreated controls (Fig. 8a). Thus the effect of FGF-2 withdrawal on hESC becomes manifest only gradually.

At day 7 the absence of FGF-2 had marginal effects on hESC morphology, with some colonies developing disorganized edges (Figs. 8b and 8c). By day 15, untreated colonies appeared mostly differentiated, with extensive areas of cyst formation compared to FGF-2 treated colonies (Figs. 8d and 8e). Quantitative flow-cytometric analysis confirmed these observations (Fig. 8f). As expected, on day 7 GCTM-2 labeling profiles were not significantly different with (63 ± 1.9%) or without FGF-2 treatment (59 ± 0.8%). However, at 15 days, FGF-2 significantly increased (66 ± 4.1%) the proportion of GCTM-2-positive cells over untreated cells (39 ± 7.5%). Thus, FGF-2 is not critical for short-term ES cell propagation

Figure 8 (a) With FGF-2 treatment, cell number at experimental day 15 was significantly (**$p<0.01$) higher compared to untreated cells. Dotted line represents control levels in the absence of FGF-2 arbitrarily set to 1. HESC colonies at day 7 show (b) tight colony morphology and no differentiation in the presence of FGF-2 and (c) minimal differentiation and slight distortion of colony edges without FGF-2 treatment. HESC colonies at day 15 show (d) minimal differentiation in the center of the colony and preservation of defined edges with FGF-2 treatment and (e) loss of ES cell colony morphology and widespread cystic and differentiated areas without defined colony borders in the absence of FGF-2. Scale bars, 100 μm. (f) Flow-cytometric profiles of GCTM-2 expression showing that cells treated with FGF-2 were less differentiated at days 7 and 15 than untreated cells. Statistical analysis of three independent experiments confirmed that the effect at day 15 was significant ($p<0.01$). To determine the effects of FGF-2 on cell proliferation or apoptosis, cells for each treatment were analyzed with flow-cytometric immunoassays and subdivided into groups according to GCTM-2 expression intensity, ranging in percentile intervals from 20 to 100. Cells treated and untreated with FGF-2 were analyzed for cell cycle structure, showing the proportions of cells in G_0/G_1, S, and G_2/M phases at (g) day 7 of culture and (h) day 15 of culture, and (i) apoptosis assayed by the TUNEL method at day 15. Significant differences are indicated by asterisks (*$p<0.05$ or **$p<0.01$).

although its inhibitory effect on spontaneous differentiation is necessary to maintain ES cells in serum-free culture for prolonged periods.

We also examined the effects of FGF-2 on the cell cycle profiles of cell subpopulations with different GCTM-2 expression levels. After 7 days of culture in the absence of FGF-2, cell cycle profiles across the entire GCTM-2 labeling distribution were not significantly different from those of treated cells (Fig. 8g). By day 15 a moderate but significantly higher proliferative fraction was observed in GCTM-2^{NEG} (first quintile) cells and GCTM-2^{LOW} cells in the second and third quintiles (13%) in the presence of FGF-2 (Fig. 8h). By contrast growth factor treatment did not exert a mitogenic effect on GCTM-2^{HIGH} cells (fifth quintile) at day 15. GCTM-2^{NEG} cells showed a reduced proliferative fraction at day 15 compared to day 7. This reduction was more than twofold greater for untreated cells (27%) than for those stimulated by FGF-2 (13%) (Fig. 8h).

In light of the increased cell number observed and proportion of GCTM-2-positive cells in the presence of FGF-2, we examined if the factor inhibited apoptosis by a flow-cytometric immunoassay detecting DNA fragmentation as part of the apoptotic program by the terminal deoxynucleotidyltransferase dUTP nick-end labeling (TUNEL) method. As a positive control, short-wave UV treatment of hESC cultures caused a 2.5-fold increase in apoptosis to be detected by this method (not shown). Cells grown for 15 days in the presence or absence of FGF-2 were compared for apoptotic cell rates across GCTM-2 expression (Fig. 8i). The significant increases in cell number and amount of GCTM-2-positive cells at day 15 were not due to an antiapoptotic effect elicited by FGF-2 stimulation. The level of apoptosis at this time interval remained relatively unchanged under both treated (21 ± 2.7) and untreated (21 ± 2.6) conditions over the entire GCTM-2 distribution.

Discussion

Spontaneous differentiation occurs under most hESC growth conditions, producing a heterogeneous culture. To conduct accurate and unambiguous cell cycle analyses we fractionated the hESC population using an antibody recognizing a cell surface marker (GCTM-2) of undifferentiated hESC. GCTM-2^{HIGH} cells showed the highest proliferative and lowest G_0/G_1 cell cycle fraction. GCTM-2^{LOW} or GCTM-2^{NEG} cells displayed progressively lower proliferation fractions and conversely higher proportions of cells in G_0/G_1. Complementary double flow cytometry analysis showed that GCTM-2^{HIGH} cells best represented a homogeneous subpopulation uniformly expressing Oct-4 and other markers of pluripotency. Cell populations with lower levels of the marker were progressively more contaminated with cells negative for Oct-4. Consequently, analyses of key cell cycle components in hESC were performed on GCTM-2^{HIGH} or Oct-4-positive cells.

Human Oct-4-positive cells did not express cyclin D1, D2, or D3 at the protein level and accordingly, treatment with the CDK-4 inhibitor 1,4-dimethoxy-9-thio(10*H*)-acridone did not affect the cell cycle distribution of the GCTM-2^{HIGH} cell subpopulation. The repression of D-type cyclins may be necessary for the maintenance of an undifferentiated phenotype in hESC. In the mouse embryo, expression of cyclins D1, D2, and D3 is established prior to the onset of gastrulation and correlates with lineage-specific commitment (Wianny et al., 1998; Ciemerych et al., 2002). However, cyclin D1 was cited as a pluripotent-specific gene in hESC microarray publications (Sato et al., 2003; Rao et al., 2004). Cyclin D2 and CDK-4 were also recently found to be highly expressed in hESC (Becker et al., 2006, 2007). However, these studies used a heterogeneous mixture of hESC and differentiated cells for analysis and examined global expression of mRNA, not protein at the single-cell level, as in this study.

Only after the loss of Oct-4 and the onset of differentiation does cyclin D1, D2, and D3 expression become evident. In accord with the role of D-type cyclins as growth factor-responsive catalysts for G1 progression in somatic cells (Bartek et al., 1996), we found that only cells negative for Oct-4 expression became responsive to mitogenic stimulation by FGF-2. Undifferentiated hESC do not respond to FGF-2 with a change in their cell cycle profile, and the factor has no influence on their survival. Instead FGF-2 inhibits hESC differentiation. Our data are consistent with findings from previous reports investigating the direct and/or indirect roles of this growth factor on hESC, although the examination of FGF-2-dependent effects on the rate of stem cell division or apoptosis is novel in our study (Xu et al., 2005; Kim et al., 2005; Greber et al., 2007).

Surprisingly, the cell cycle characteristics of hESC appear to be unlike those described for mouse ES cells (Savatier et al., 1994, 2002), epiblast cells (Mac Auley et al., 1993), embryonic germ cells (Resnick et al., 1992), and embryonal carcinoma cells (Mummery et al., 1987), in which DNA replication and mitotic division occur in rapid succession without fully formed gap phases. In mESC, these features have been attributed to high levels of cell-cycle-independent cyclin E/CDK-2, cyclin A/CDK-2 kinase activities, which drive proliferation and ensure the permanent inactivation of pRb protein (Stead et al., 2002). While cyclin E activity is permanent in hESC, cyclin A is expressed periodically. When resolved against cell cycle phases by flow cytometry, cyclin A upregulation was consistent with its requirement for S-phase traverse and peak activity at prometaphase allowing mitotic entry (Yam et al., 2002) in both GCTM-2^{HIGH} and GCTM-2^{NEG} cells.

The downregulation of cyclin A in the G_1 phase of hESC may lower CDK-2 kinase activity to a level acceptable for a "restriction-point-like" pRb activation event, shown to occur by coimmunostaining and immunoblot analyses. The active form of this tumor suppressor is a growth-inhibitory brake mechanism (Weinberg, 1995) and maintains cells in G_1 by repressing the transcription of S-phase-promoting genes (Ludlow et al., 1993; Harbour and Dean, 2000). We propose that G_1-specific activation of pRb is responsible for the significantly larger G_1 fraction observed in GCTM-2^{HIGH} cells compared to SSEA-1^{HIGH} cells. Interestingly, the loss of SSEA-1 did not correlate with significant changes in cell cycle structure. Consistent with our findings, mESC, both positive and negative for SSEA-1, injected into eight-stage mouse embryos still differentiate into epiblast cells in high numbers (Furusawa et al., 2004) and the loss of SSEA-1 *in vitro* was not always shown to associate with the extent of cell differentiation (Cui et al., 2004).

HESC appear dependent on cyclin A to bolster CDK-2 kinase activity and initiate G_1-S traverse by rephosphorylating pRb, but what is the likely function of a pRb-dependent G_1 checkpoint in these cells? HESC differentiation resulted in lower cyclin E/A expression and the exaggeration of G_1 coupled with the presence of active pRb in the majority of hESC marker-negative cells. The activation of pRb in cooperation with extrinsic signals has been shown to promote fate determination of neural stem cells (Jori et al., 2007) and to control strictly the lineage commitment and differentiation of progenitors in muscle, heart, and blood (reviewed in Goodrich, 2006; Galderisi et al., 2006). The G_1-specific pRb activation event was a potential divergence point at which hESC could be directed toward differentiation over self-renewal.

We speculated that if the compromise of CDK-2 kinase activity in hESC would delay these cells at the G_1-S border and increase the expression of active pRb, it may also promote the induction of differentiation. Treatment with the CDK-2 inhibitor RV resulted in the appearance of smaller "dwarf" hESC colonies and produced a twofold increase in GCTM-2^{HIGH} cells in G_1. We also observed a significant decrease in the proportion of GCTM-2^{HIGH} cells in M phase, consistent with findings indicating the importance of cyclin A/CDK-2 for S-phase progression and entry into mitosis (reviewed in Yam et al., 2002). Our triple staining and confocal imaging analyses showed that the proportion of G_1-residing, active pRb-expressing cells positive for GCTM-2 that lost Oct-4 expression was 2.5-fold higher in hESC subjected to CDK-2-dependent cell cycle delay. G_1 perturbation and prolonged pRb activation appeared to promote the disappearance of Oct-4, a stem cell marker essential for the maintenance of pluripotency that is lost with the onset of differentiation in mESC and hESC (reviewed in Pesce et al., 1999; Pesce and Scholer, 2000; Pera et al., 2000; Carpenter et al., 2003). Interestingly, the GCTM-2^{+}/Oct-4 $^{\text{and minus;}}$ cells were found previously only in the GCTM-2^{LOW} and GCTM-2^{NEG} subpopulations displaying significantly higher G_1- and lower S-phase contents compared to GCTM-2^{HIGH} cells. Given these observations one cannot exclude the possibility that CDK-2, which has broad activity throughout the cell cycle, may also regulate self-renewal by mechanisms unrelated to G_1/S control.

However, G_1 elongation and prolonged pRb activation in hESC shown here to associate with the loss of Oct-4 are likely to be a signaling mechanism for extrinsic factors to initiate early differentiation in hESC. Proteins known to differentiate hESC, like BMP-2 (Pera et al., 2004; Pal and Khanna, 2007), can elevate cyclin-dependent kinase inhibitor p21Cip1, downregulating CDK-2 activity and promoting pRb activation in cells (Ghosh-Choudhury et al., 2000). The link between p21 upregulation, pRb activation, and cell differentiation is in turn firmly established during lineage commitment in blood and muscle (reviewed in Kitzmann and Fernandez, 2001; Steinman, 2002; Furukawa, 2002).

These data provide the first evidence whereby the perturbation of G_1 and consequently the prolonged activation of pRb provide the necessary signals to initiate the onset of hESC differentiation. Our results are in agreement with accumulating evidence showing active pRb as a master regulator required for the induction of tissue-specific gene expression during the early differentiation of various cell lineages (reviewed in De Falco et al., 2006; Skapek et al., 2006). We propose that the active pRb checkpoint in the hESC G_1 is also a control point for the initiation of differentiation, commitment, and conversion to a conventional mode of cell cycle control found in somatic cells.

Materials and methods

Cell culture and treatments

The derivation and routine culture of the stocks of HES-2, HES-3, and HES-4 cell lines were previously described (Reubinoff et al., 2000). To produce larger numbers of cells required for these experiments, hESC were grown on mitomycin-treated MEF in the presence of 80% Dulbecco's modified Eagles medium F-12 formulation (Invitrogen, CA, USA), 0.1 mM β-mercaptoethanol, 1% nonessential amino acids, 2 mM L-glutamine, and 20% KnockOut SR serum replacer medium (Gibco BRL). Culture medium was supplemented with human recombinant FGF-2 (4 ng/ml) (Amit et al., 2000). Cells were passaged by enzymatic dissociation using Collagenase IA (1 mg/ml) (Sigma-Aldrich, MO, USA) and mechanical shearing of whole ES cell colonies for large-scale propagation. The pharmacological CDK-2 inhibitor Roscovitine (30 μM, IC_{50} 700 nM), pharmacological CDK-4 inhibitor II (10 μM, IC_{50} 200 nM), or DMSO control solutions were administered into culture media 24 h after hESC subculture and replenished daily with medium changes for 6 days of growth before cell cycle analyses. OKO mouse ES cells used for this study were cultured on 0.1% gelatin in 80% Dulbecco's modified Eagles medium (Invitrogen), 0.1 mM β-mercaptoethanol, 1% nonessential amino acids, 2 mM L-glutamine, and 20% bovine serum (Gibco BRL). The medium was supplemented with LIF (10 ng/ml).

BrdU proliferation assay

HES-2 and HES-4 cells were incubated with 1:1000 BrdU labeling reagent (Roche, Mannheim, Germany) for 2 h at 37 °C and 5% CO_2. HESC were harvested as mentioned above and dissociated into single-cell suspension with trypsin (0.5 mg/ml), fixed in 100% methanol for 1 h, and denatured in 4 N HCl for 10 min. The acidic solution was neutralized by repeatedly washing cells with fetal calf serum (FCS) (Hyclone, UT, USA)-containing medium. The cells were then labeled with GCTM-2 indirectly conjugated to allophycocyanin and then anti-BrdU antibody directly conjugated to FLUOS (Roche) and finally counterstained with propidium iodide (2 μg/ml). An aliquot of cells was retained to measure the extent of MEF feeder cells in sample material using anti-mouse Thy1.2 directly conjugated to phycoerythrin. The cells were analyzed on a MoFlo flow cytometer using Summit v3.1 sort control software.

TUNEL apoptotic assay

HES-2, HES-3, and HES-4 cells colonies were harvested and dissociated into single-cell suspension as mentioned above. Fixation of the cells was performed in 1% paraformaldehyde for 15 min on ice followed by a PBS wash and refixation in 70%

ethanol for 24 h at −20 °C. Cells were washed free of the fixative in PBS and treated with a TUNEL reaction solution for 1 h at 37 °C prepared according to the manufacturer's instructions (Pharmingen, NJ, USA). TUNEL-positive cells were stained by a fluorescein-conjugated antibody supplied in the reaction solution. The cells were then labeled with GCTM-2 indirectly conjugated to Alexa-Fluor 647 (Molecular Probes, OR, USA). The extent of MEF contamination and the flow-cytometric analysis were performed as described above.

Immunofluorescence

Cells grown on slides were fixed and permeabilized with 100% ethanol, 100% methanol, or acetone/H_2O 9/1 and immunostained with antibodies raised against the following stem cell markers as described previously (Pera et al., 2003): GCTM-2 (this laboratory), TRA-1-60 (gift from P. Andrews, University of Sheffield), SSEA-1 (Developmental Studies Hybridoma Bank), and Oct-4 (Santa Cruz Biotechnology, CA, USA). Cell cycle analysis was conducted using antibodies raised against cyclin D1 (DCS-6) and underphosphorylated retinoblastoma protein (G99-549) (Pharmingen); cyclin D2 (34B1-3), cyclin D3 (18B6-10), and cyclin E (M-20) (all from Santa Cruz Biotechnology); cyclin A (mouse IgG1) and hyperphosphorylated (Ser 795) retinoblastoma protein (Cell Signaling Technology, MA, USA); and cyclin A (mouse IgG2a) (Sigma). Secondary antibody fluorochromes used were FITC, Cy3, and Cy5 (Jackson Immunoresearch); and Alexa-Fluor-350, Alexa-Fluor-488, and Alexa-Fluor-568. Where required, nuclei were counterstained with Hoechst 33342 (Chemicon, CA, USA) and specimens mounted using antifading solution (Vectashield, Australia). Specificity of immunoreagents was verified by the absence of staining in isotype-specific negative controls. Photographic images were captured at 20 °C using immunofluorescence or phase-contrast microscopy using an upright Leica DMR microscope equipped with a mercury arc lamp. The objectives used were a 20 and times; phase with a numerical aperture (na = 0.60), a 40× phase objective (na = 0.75), and a 63× oil immersion objective (na = 1.32). Image files were saved in TIFF format on a Leica DC200 photographic program or Leica SP2 AOBS confocal imaging software (Mannheim, Germany) and uniformly adjusted alongside control images for appropriate viewing brightness or contrast with Adobe PhotoShop v5.5 image software. Quantitation of fluorescently stained cells was performed on three replicate slides for each experiment by counting at least 500 cells per slide in each fluorescence channel.

FACS analysis and cell sorting

Cells were dissociated into single-cell suspension as previously described and immunostained live for GCTM-2 or fixed and permeabilized with 100% methanol for Oct-4 labeling. Antibodies raised to GCTM-2 or Oct-4 were applied (100 μl antibody/10^6 cells), and the cells were labeled on ice for 30 min, washed with FCS-containing medium, and incubated on ice for 30 min with an FITC-conjugated secondary antibody (Dako, Glostrup, Denmark). Cells sorted on the basis of GCTM-2 fluorescence intensity were collected in plastic ampoules, filled with FCS-containing medium to minimize cell lysis, and stored immediately on ice until lysis treatment.

Western blot analysis

GCTM-2^{HIGH} HES-3 cells were lysed with RIPA lysis buffer (10 mM Tris-HCl, pH 7.5, 150 mM NaCl, 1% deoxycholate, 1% Triton X-100, protease inhibitor tablet Cocktail II 1:10 from Roche, 0.4 mM NaF, 0.4 mM $NaVO_4$, 0.1 mM EDTA, 0.1 mM EGTA, 7.5 μg/ml aprotinin, 70 μg/ml PMSF) for 5 min at 4 °C. The lysate was clarified by centrifugation at 14,000*g* for 10 min at 4 °C and protein concentrations were determined by Bradford assay using a Bio-Rad kit. Equal lysate volumes were combined with 2×reducing loading buffer before the sample was denatured for 5 min in a boiling water bath. Cell lysates were resolved on a 6% SDS Tris-glycine polyacrylamide gel and electrotransferred to PVDF membranes, which were blocked in 5% skim milk, 0.1% Tween 20 for 3 h at room temperature or overnight at 4 °C. Membranes were incubated for 2 h with retinoblastoma antibodies (G99-549 or Ser 795) at room temperature, washed four times with PBS containing 0.1% Tween 20 (PBST), and incubated for 1 h with a horseradish peroxidase (HRP)-conjugated secondary antibody (Dako) in PBST. HRP activity was detected with an ECL detection kit (Amersham, Buckinghamshire, UK) on Kodak film.

Statistical analysis

Experiments were performed at least three times. Data were analyzed as the means ± SD of at least three independent experiments.

Acknowledgments

The authors thank technical staff, for supplying cell material and reagents vital to this study, as well as all group members for their input, with particular thanks to Paul Hutchinson for flow-cytometric expertise. We also thank Dr. Souheir Houssami, who provided guidance in the preliminary stages of these experiments. This work was supported by grants from the National Health and Medical Research Council (Australia), the National Institutes of Health (USA) (GM 068417-01), and the Bsik Programme "Stem Cells in Development and Disease."

Appendix A. Supplementary data

Supplementary data associated with this article can be found, in the online version, at doi:10.1016/j.scr.2007.09.002.

References

Amit, M., Carpenter, M.K., Inokuma, M.S., Chiu, C.P., Harris, C.P., Waknitz, M.A., Itskovitz-Eldor, J., Thomson, J.A., 2000. Clonally derived human embryonic stem cell lines maintain pluripotency and proliferative potential for prolonged periods of culture. Dev. Biol. 227, 271–278.

Bartek, J., Lukas, J., Bartkova, J., 1996. Perspective: defects in cell cycle control and cancer. J. Pathol. 187, 95–99.

Becker, K.A., Ghule, P.N., Therrien, J.A., Lian, J.B., Stein, J.L., van Wijnen, A.J., Stein, G.S., 2006. Self-renewal of human embryonic stem cells is supported by a shortened G1 cell cycle phase. J. Cell. Physiol. 209, 883–893.

Becker, K.A., Stein, J.L., Lian, J.B., van Wijnen, A.J., Stein, G.S., 2007. Establishment of histone gene regulation and cell cycle checkpoint control in human embryonic stem cells. J. Cell. Physiol. 210, 517–526.

Buchkovich, K., Duffy, L.A., Harlow, E., 1989. The retinoblastoma protein is phosphorylated during specific phases of the cell cycle. Cell 58, 1097–1105.

Carpenter, M.K., Rosler, E., Rao, M.S., 2003. Characterization and differentiation of human embryonic stem cells. Cloning Stem Cells 5, 79–88.

Ciemerych, M.A., Kenney, A.M., Sicinska, E., Kalaszczynska, I., Bronson, R.T., Rowitch, D.H., Gardner, H., Sicinski, P., 2002. Development of mice expressing a single D-type cyclin. Genes Dev. 16, 3277–3289.

Classon, M., Harlow, E., 2002. The retinoblastoma tumor suppressor in development and cancer. Nat. Rev. Cancer 2, 910–917.

Cui, L., Johkura, K., Yue, F., Ogiwara, N., Okouchi, Y., Asanuma, K., Sasaki, K., 2004. Spatial distribution and initial changes of SSEA-1 and other cell adhesion-related molecules on mouse embryonic stem cells before and during differentiation. J. Histochem. Cytochem. 52, 1447–1457.

De Falco, G., Comes, F., Simone, C., 2006. pRb: master of differentiation. Coupling irreversible cell cycle withdrawal with induction of muscle-specific transcription. Oncogene 25, 5244–5249.

Draper, J.S., Smith, K., Gokhale, P., Moore, H.D., Maltby, E., Johnson, J., Meisner, L., Zwaka, T.P., Thomson, J.A., Andrews, P.W., 2004. Recurrent gain of chromosomes 17q and 12 in cultured human embryonic stem cells. Nat. Biotechnol. 22, 53–54.

Dvorak, P., Dvorakova, D., Koskova, S., Vodinska, M., Najvirtova, M., Krekac, D., Hampl, A., 2005. Expression and potential role of fibroblast growth factor 2 and its receptors in human embryonic stem cells. Stem Cells 23, 1200–1211.

Fluckiger, A.C., Marcy, G., Marchand, M., Negre, D., Cosset, F.L., Mitalipov, S., Wolf, D., Savatier, P., Dehay, C., 2006. Cell cycle features of primate embryonic stem cells. Stem Cells 24, 547–556.

Furukawa, Y., 2002. Cell cycle control genes and hematopoietic cell differentiation. Leuk. Lymphoma 43, 225–231.

Furusawa, T., Ohkoshi, K., Honda, C., Takahashi, S., Tokunaga, T., 2004. Embryonic stem cells expressing both platelet endothelial cell adhesion molecule-1 and stage-specific embryonic antigen-1 differentiate predominantly into epiblast cells in a chimeric embryo. Biol. Reprod. 70, 1452–1457.

Galderisi, U., Cipollaro, M., Giordano, A., 2006. The retinoblastoma gene is involved in multiple aspects of stem cell biology. Oncogene 25, 5250–5256.

Ghosh-Choudhury, N., Woodruff, K., Qi, W., Celeste, A., Abboud, S.L., Ghosh Choudhury, G., 2000. Bone morphogenetic protein-2 blocks MDA MB 231 human breast cancer cell proliferation by inhibiting cyclin-dependent kinase-mediated retinoblastoma protein phosphorylation. Biochem. Biophys. Res. Commun. 272, 705–711.

Goodrich, D.W., 2006. The retinoblastoma tumor-suppressor gene, the exception that proves the rule. Oncogene 25, 5233–5243.

Greber, B., Lehrach, H., Adjaye, J., 2007. Fibroblast growth factor 2 modulates transforming growth factor beta signaling in mouse embryonic fibroblasts and human ESCs (hESCs) to support hESC self-renewal. Stem Cells 25, 455–464.

Harbour, J.W., Dean, D.C., 2000. The Rb/E2F pathway: expanding roles and emerging paradigms. Genes Dev. 14, 2393–2409.

Jori, F.P., Galderisi, U., Napolitano, M.A., Cipollaro, M., Cascino, A., Giordano, A., Melone, M.A., 2007. RB and RB2/P130 genes cooperate with extrinsic signals to promote differentiation of rat neural stem cells. Mol. Cell. Neurosci. 34, 299–309.

Juan, G., Gruenwald, S., Darzynkiewicz, Z., 1998. Phosphorylation of retinoblastoma susceptibility gene protein assayed in individual lymphocytes during their mitogenic stimulation. Exp. Cell Res. 239, 104–110.

Khidr, L., Chen, P.L., 2006. RB, the conductor that orchestrates life, death and differentiation. Oncogene 25, 5210–5219.

Kim, S.J., Cheon, S.H., Yoo, S.J., Kwon, J., Park, J.H., Kim, C.G., Rhee, K., You, S., Lee, J.Y., Roh, S.I., Yoon, H.S., 2005. Contribution of the PI3K/Akt/PKB signal pathway to maintenance of self-renewal in human embryonic stem cells. FEBS Lett. 579, 534–540.

Kitzmann, M., Fernandez, A., 2001. Crosstalk between cell cycle regulators and the myogenic factor MyoD in skeletal myoblasts. Cell. Mol. Life Sci. 58, 571–579.

Ludlow, J.W., Glendening, C.L., Livingston, D.M., DeCarprio, J.A., 1993. Specific enzymatic dephosphorylation of the retinoblastoma protein. Mol. Cell. Biol. 13, 367–372.

Mac Auley, A., Werb, Z., Mirkes, P.E., 1993. Characterization of the unusually rapid cell cycles during rat gastrulation. Development 117, 873–883.

Mummery, C.L., van den Brink, C.E., de Laat, S.W., 1987. Commitment to differentiation induced by retinoic acid in P19 embryonal carcinoma cells is cell cycle dependent. Dev. Biol. 121, 10–19.

Pal, R., Khanna, A., 2007. Similar pattern in cardiac differentiation of human embryonic stem cell lines, BG01V and ReliCellhES1, under low serum concentration supplemented with bone morphogenetic protein-2. Differentiation 75, 112–122.

Pera, M.F., Trounson, A.O., 2004. Human embryonic stem cells: prospects for development. Development 131, 5515–5525.

Pera, M.F., Reubinoff, B., Trounson, A., 2000. Human embryonic stem cells. J. Cell Sci. 113, 5–10.

Pera, M.F., Filipczyk, A.A., Hawes, S.M., Laslett, A.L., 2003. Isolation, characterization, and differentiation of human embryonic stem cells. Methods Enzymol. 365, 429–446.

Pera, M.F., Andrade, J., Houssami, S., Reubinoff, B., Trounson, A., Stanley, E.G., Wardvan Oostwaard, D., Mummery, C., 2004. Regulation of human embryonic stem cell differentiation by BMP-2 and its antagonist noggin. J. Cell Sci. 117, 1269–1280.

Pesce, M., Scholer, H.R., 2000. Oct-4: control of totipotency and germline determination. Mol. Reprod. Dev. 55, 452–457.

Pesce, M., Anastassiadis, K., Scholer, H.R., 1999. Oct-4: lessons of totipotency from embryonic stem cells. Cells Tissues Organs 165, 144–152.

Rao, R.R., Calhoun, J.D., Qin, X., Rekaya, R., Clark, J.K., Stice, S.L., 2004. Comparative transcriptional profiling of two human embryonic stem cell lines. Biotechnol. Bioeng. 88, 273–286.

Resnick, J.L., Bixler, L.S., Cheng, L., Donovan, P.J., 1992. Long-term proliferation of mouse primordial germ cells in culture. Nature 359, 550–551.

Reubinoff, B.E., Pera, M.F., Fong, C.Y., Trounson, A., Bongso, A., 2000. Embryonic stem cell lines from human blastocysts: somatic differentiation in vitro. Nat. Biotechnol. 18, 399–404.

Sato, N., Sanjuan, I.M., Heke, M., Uchida, M., Naef, F., Brivanlou, A.H., 2003. Molecular signature of human embryonic stem cells and its comparison with the mouse. Dev. Biol. 260, 404–413.

Savatier, P., Huang, S., Szekely, L., Wiman, K.G., Samarut, J., 1994. Contrasting patterns of retinoblastoma protein expression in mouse embryonic stem cells and embryonic fibroblasts. Oncogene 9, 809–818.

Savatier, P., Lapillonne, H., van Grunsven, L.A., Rudkin, B.B., Samarut, J., 1996. Withdrawal of differentiation inhibitory activity/leukemia inhibitory factor up-regulates D-type cyclins and cyclin-dependent kinase inhibitors in mouse embryonic stem cells. Oncogene 12, 309–322.

Savatier, P., Lapillonne, H., Jirmanova, L., Vitelli, L., Samarut, J., 2002. Analysis of the cell cycle in mouse embryonic stem cells. Methods Mol. Biol. 185, 27–33.

Skapek, S.X., Pan, Y.R., Lee, E.Y., 2006. Regulation of cell lineage specification by the retinoblastoma tumor suppressor. Oncogene 25, 5268–5276.

Smith, A.G., Heath, J.K., Donaldson, D.D., Wong, G.G., Moreau, J., Stahl, M., Rogers, D., 1988. Inhibition of pluripotential embryonic stem cell differentiation by purified polypeptides. Nature 336, 688–690.

Stead, E., White, J., Faast, R., Conn, S., Goldstone, S., Rathjen, J., Dhingra, U., Rathjen, P., Walker, D., Dalton, S., 2002. Pluripotent cell division cycles are driven by ectopic Cdk2, cyclin A/E and E2F activities. Oncogene 21, 8320–8333.

Steinman, R.A., 2002. Cell cycle regulators and hematopoiesis. Oncogene 21, 3403–3413.

Thomson, J.A., Itskovitz-Eldor, J., Shapiro, S.S., Waknitz, M.A., Swiergiel, J.J., Marshall, V.S., Jones, J.M., 1998. Embryonic stem cell lines derived from human blastocysts. Science 282, 1145–1147.

Weinberg, R.A., 1995. The retinoblastoma protein and cell cycle control. Cell 81, 323–330.

Wianny, F., Real, F.X., Mummery, C.L., Van Rooijen, M., Lahti, J., Samarut, J., Savatier, P., 1998. G1-phase regulators, cyclin D1, cyclin D2, and cyclin D3: up-regulation at gastrulation and dynamic expression during neurulation. Dev. Dyn. 212, 49–62.

Williams, R.L., Hilton, D.J., Pease, S., Willson, T.A., Stewart, C.L., Gearing, D.P., Wagner, E.F., Metcalf, D., Nicola, N.A., Gough, N. M., 1988. Myeloid leukaemia inhibitory factor maintains the developmental potential of embryonic stem cells. Nature 336, 684–687.

Xu, R.H., Peck, R.M., Li, D.S., Feng, X., Ludwig, T., Thomson, J.A., 2005. Basic FGF and suppression of BMP signaling sustain undifferentiated proliferation of human ES cells. Nat. Methods 2, 185–190.

Yam, C.H., Fung, T.K., Poon, R.Y., 2002. Cyclin A in cell cycle control and cancer. Cell. Mol. Life Sci. 59, 1317–1326.

Zarkowska, T., Mittnacht, S., 1997. Differential phosphorylation of the retinoblastoma protein by G1/S cyclin-dependent kinases. J. Biol. Chem. 272, 12738–12746.